Constraining historical black carbon emission inventory of United States for 1960s-2000s

Tianye Sun, Liang Liu, Tami C Bond, Mark Flanner, Thomas W. Kirchstetter, Chaoyi Jiao, Chelsea V. Preble, Wayne Chang

ABSTRACT

To improve the accuracy of black carbon emission inventory of US for 1960s to 2000s, we studied the relationship between emissions and ambient air concentrations of BC using the Community Atmosphere Model and formulated it into matrices that allow reconstruction of BC ambient concentration with emission inventory. Errors in model meteorology are corrected in the transport matrices by adjustment with measurements from NASA. We also applied Heating Degree Days data to estimate seasonal variation in emissions, as observed from the concentrations. Comparison between the reconstructed and measured BC shows that the magnitude of observations was decreasing throughout this period of time, while the reconstructed concentrations peaked in the 1980s. Also, scaling heating emissions by HDD can explain most of the trend in seasonal variation observed in the measurements. Acknowledging the inherent uncertainty in model-measurement comparison, we rely more on the trends comparison. Apparent adjustment factors are calculated for baseline and seasonal emissions for each decade. To reproduce the decreasing trend, higher emission factors are needed for 1960s to 1970s. More information is required to further improve the emission inventory on fuel consumption and technology level.

INTRODUCTION

Black carbon (BC) is a kind of carbonaceous particle produced by incomplete combustion of carbon-based fuel [1-3]. It influences the regional and global climate by absorbing visible light and warming the atmosphere [4-7]. The best estimate of industrial-era climate forcing of black carbon through all forcing mechanisms is 1.1 W/m2 [1]. However, climate forcing from BC is transient due to its short lifetime [5, 8, 9]. Therefore, reducing black carbon could present quicker climate benefits than mitigating greenhouse gas with much longer lifetimes. To better explore the environmental consequences of black carbon, confidence in its emission inventory is important. In this work, we use historical BC measurements to constrain seasonal and baseline BC emissions for 1960s to 2000s. When there is a mismatch between models and measurements, and the emission inventory is at fault, an error in estimated fuel use or technology is implied. This in turn will ultimately affect emission estimates of all pollutants. Thus, the annual and seasonal trend in observations of BC will constrain our current representation of fuel use and emission factors and then provide more accurate emissions of BC and other species.

METHODOLOGY

To improve the accuracy of historical BC emission estimation based on observations, we interpreted the emission into observable variables and compared them with observations. Then, we analyzed the discrepancy between the modeled concentrations and its measurements. The flow chart in **Figure 1** describes the calculation process. There are three main steps of the method as described by the following sections.
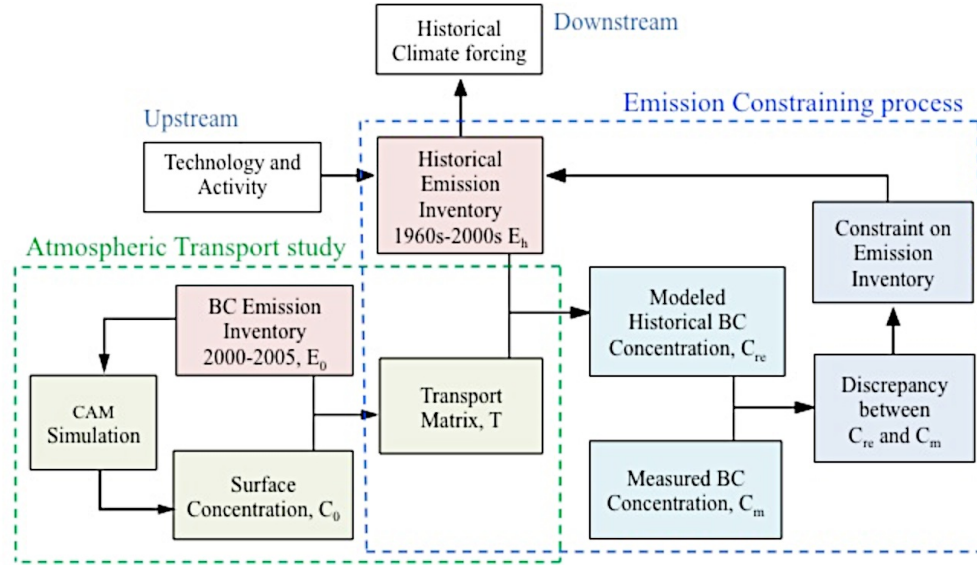
Figure 1. Flowchart of the method

Step One. Atmospheric transport study

1.1 Calculation of the transport matrix

First, we simulated atmospheric transport over the period of 2000-2006 using a special version of NCAR Community Atmospheric Model (CAM) version 4.0 that tracks BC tracers from different sources as different "species". The simulation ran with 1.9×2.5 degree grid boxes, forced with transient sea surface temperatures and with the emission inventory reported by Bond, Bhardwaj [2]. Using the model simulation result, we formulated the relationship between emissions and ambient air concentration into transport matrices. Each element, T_{ij}, in the transport matrix represents the sensitivity of ambient air concentration in a receptor region i to the emission in source region j, The transport matrix is the m×k matrix transferring the vector of k regional emissions $\vec{E}$ into the concentration vector $\vec{C}$ of m receptors:

Equation (1) $$\vec{C} = T\vec{E}$$

The concept and function of our transport matrix is same as the Jacobian matrix in the inverse modeling method [10]. In this study, as in inverse modeling studies, we assume this relationship is linear and independent of the magnitude of emission.

The transport matrices were calculated monthly to account for seasonal variation. In this study, we assume that the dominant BC contribution to each receptor is emissions within the same state. The full transport matrices are shown in supplementary information.

1.2 Error of meteorology in the model

Errors in model meteorology could cause discrepancy between estimation and measurements, which should not be attributed to the inaccuracy of the emission inventory. We examine the influence of planetary boundary layer (PBL) and wind speed on BC concentrations. We found that only PBL is a statistically significant predictor of BC concentration. These different statistical results for PBL and wind are physical plausible. The grid box in this simulation is as big as 1.9x2.5 degree that equilibrium concentration of the region is not dominated by the local wind speed. It is the total emission dispersion rather than certain emission source that influence the BC concentrations in large scale. This is similar to

the case that rural BC concentrations in remote site do not change with local wind speed [11]. Therefore, little correlation between BC concentration and wind speed is observed. Then, we compared the planetary boundary layer (PBL) in the model with measurements acquired from NASA's Modern-Era Retrospective Analysis for Research and Applications (MERRA) for the period 2000-2006. Figure 2 shows the comparison of modeled and measured PBL in the Bay Area of California (one grid box in the model). Measured and modeled values could differ by 60%. With the relationship between BC concentration and PBL from model simulation results, we can adjust the modeled BC concentrations with PBL measurements to account for the error in the model. The adjustments factors are shown in Table 1. Applying the adjusted coefficient of PBL introduces more seasonality in the concentration.

Table 1. Adjustment factor applied to BC concentration to account for the error in PBL of the model

	Jan	Feb	Mar	Apr	May	Jun	Jul	Aug	Sep	Oct	Nov	Dec
California	1.06	0.92	0.90	0.88	0.89	0.88	0.87	0.86	0.85	0.85	0.97	1.03
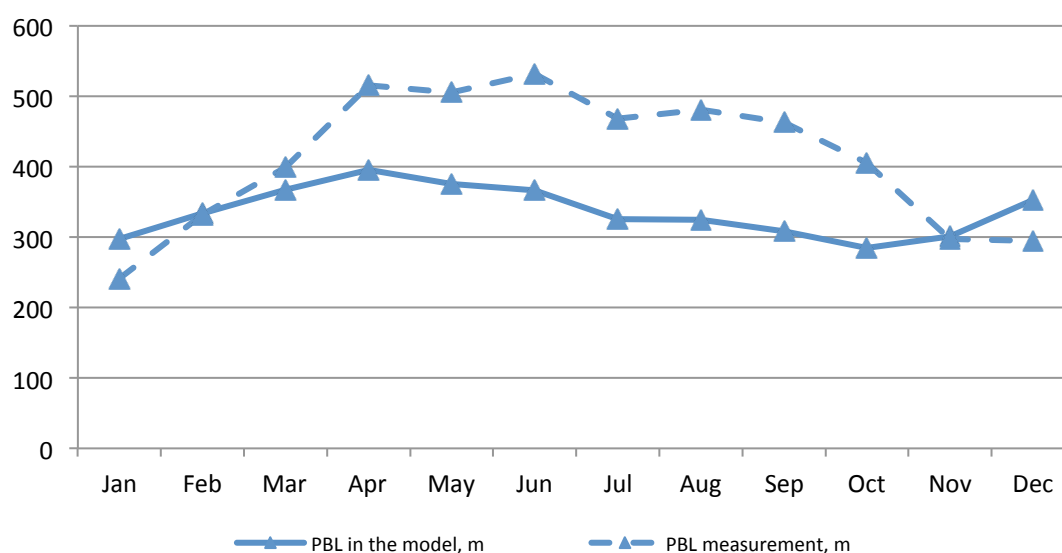
Figure 2. Monthly averages of the Planet Boundary Layers(PBL) wind speed vertical average in Bay Area of California Measurements of wind speeds and PBL for 2007-2009 are acquired from MERRA and Applications.

Step Two. Update the current emission inventory with new fuel data and seasonality data

BC concentrations were first modeled with a US BC emission inventory for 1960 to 2000 beginning with the inventory of Bond, Bhardwaj [2] with updates as described Lamarque [12]. The emission inventory used in this work has two major updates, in addition. First, United States fuel consumption data are taken from the Energy Information Administration (EIA). EIA data are disaggregated by state, whereas IEA data are given by country. The second difference is the use of the SPEW-Trend vehicle fleet model [13] to estimate the number of vehicles built according to different standards that are emitting in each year. This fleet-model approach gives a more realistic estimate of trends, because emissions do not cease when emission standards come into force, but rather when old vehicles retire from the road.

We also add seasonality into the residential sector, assuming that emission is proportional to heating degree days (HDD), which describe the heating energy used to bring a building's temperature to a desired temperature [14-16]. Equation (2) gives the definition:

Equation (2)
$$HDD = \sum_{d=1}^{n} max(T_{set} - T_d, \ 0)$$

where HDD stands for monthly degree-days; T_d is daily temperature; and T_{set} is the temperature of the indoor environment. HDD data from the National Oceanic and Atmospheric Administration (NOAA) National Climate Data Center are used to calculate a seasonality factor, as shown in Equation (3), and the monthly emission is calculated by multiplying the average residential emission with the seasonality factor. The full seasonality factors are shown in Figure S1 in the supplementary information.

Equation (3)
$$TF(HDD)_i = \frac{HDD_i}{HDD} \ \ for \ i^{th} \ month$$

Step Three. Analysis of Discrepancy between Estimation and Observation
    With the transport matrix adjusted by meteorology and the updated emission inventory, we estimated a time-dependent BC concentration of California for 1960s to 2000s and compared it with the observation. BC concentration data are estimated from COH data acquired from the California Air Resources Board (CARB) and Environmental Protection Agency's Air Quality System. The measurements of COH are similar to those of BC [17], because both are based on the quantification of light transmission through a filter upon which particles are collected [18, 19]. Equation (4) gives the conversion of COH to BC. The COH data are available for California and New Jersey during 1963-2011 and 1967-2005, respectively. They are also available for seven other states during 1965-1980 (not discussed here).

Equation (4)
$$BC \ (\mu g \ m - 3) \ = \ 6.7COH \ + \ 0.1$$

We take the observation of BC as an indication of the true emission and use the discrepancy between the modeled BC and the measurement to adjust the current emission inventory, as shown by Equation (5). Adjustment factors were calculated based on the proportions of decadal concentration average. During this process, emissions were divided into a baseline component that is constant throughout the year, and a seasonal component that varies by month. We assume seasonal emissions are from heating use, and only baseline emissions occur in summer. Therefore, summer observations were used to obtain an adjustment for baseline emissions, see Equation (6). We then calculate the adjustment to the remaining seasonal emissions. Full equations are in supplementary information.

For the ith month:

Equation (5)
$$\frac{C_{mi}}{C_{ei}} = \frac{E_b' + E_{si}'}{E_b + E_{si}} \ \ for \ i^{th} \ month$$

Equation (6)
$$\frac{C_{mi}}{C_{ei}} = \frac{E_b'}{E_b} \ \ \ \ i=6,7,8$$

where C_{mi} and C_{ei} are the measured and estimated BC concentrations for the ith month. E_b' and E_b are the true and estimated baseline emissions, respectively. E_{si}' and E_{si} are the true and estimated seasonal emissions for each month.

RESULTS and DISCUSSION

    Measured BC and modeled BC from current emission inventory and the adjusted emission for California are shown in Figure 3. After adjusting the meteorology and applying HDD seasonality, BC modeled from the initial emission inventory (red line) still shows a smaller magnitude, less seasonality and different trend than the measurements (black line). A decreasing trend is observed from BC measurement for 1960s -2000s, but not in BC modeled from the current emission inventory, which

peaks in 1980s. The modeled BC from the adjusted emission (blue line), however, matches the measurement well except for an overestimation of seasonality during the 1960s. It demonstrates that HDD can explain most of the trend in seasonal variation of the BC measurement.
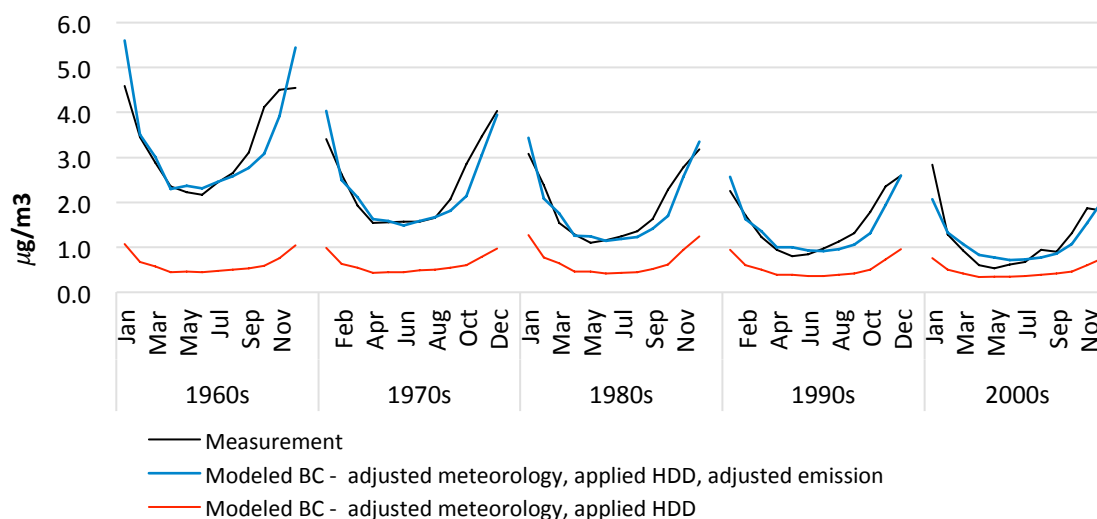
Figure 3. Measured BC and modeled BC from initial emission inventory and the adjusted emission inventory

Even though the modeled BC from the adjustment emission matches the observation well, we would not directly apply these adjustment factors on to our current emission inventory for two reasons. First, spatial heterogeneity in model-measurement comparison can cause a large uncertainty due to the difference in resolution, especially for measurements of the urban sites where concentration gradients are steep. We acknowledge the potential discrepancy caused by this resolution difference and quantified this discrepancy with a WRF-Chem model simulation of BC mass concentration over Los Angeles, California. Result shows that BC concentrations may vary by a factor of two when lower grid size from 0.04°×0.04° to 1°×1°. Therefore, the adjustment factor may be overestimated by a factor of at least two. More importantly, this spatial heterogeneity problem points out inherent uncertainty in model-measurement comparison within a model and indicates that trend comparison is more instructive. Trends in the adjustment factor are more instructive to isolate potential improvements in the emission inventory.

Figure 4 shows the apparent adjustment factors that have been divided by two to account for the resolution uncertainty. Adjustment factors for baseline emissions decrease through the study period. Although most of the mismatch in the present-day model could be explained by spatial resolution, emissions need a 2.5-fold increase in the 1960s even when resolution is accounted for. In contrast, for seasonal emission, adjustment factors are large in 1960s, 1970s, and 2000s, and relatively small in 1980s.
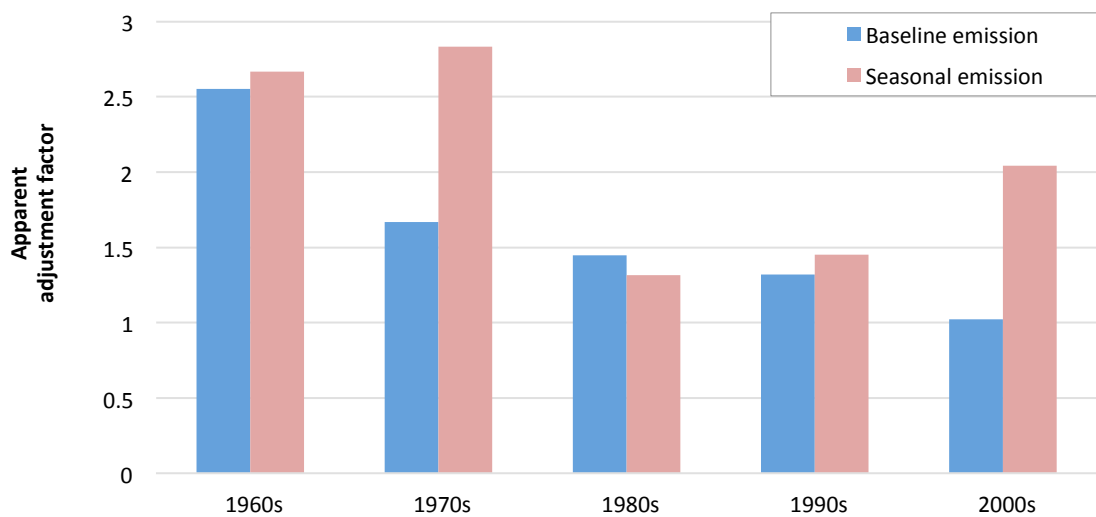
Figure 4. Apparent adjustment factors for BC emission in California

CONCLUSIONS and FUTURE WORK

To improve the accuracy of the US BC emissions for 1960s to 2000s, we translated emissions into concentrations using a transport matrix and compared them with observations. The comparison shows a mismatch of the trend between measurements and emissions. BC measurements decrease during 1960s to 2000s, but the emission inventory peaked in 1980s. Our process includes an adjustment to modeled concentrations to account for meteorology. Scaling heating emissions by HDD can explain most of the trend in seasonal variation observed in the measurements. Higher emission factors are needed for 1960s to 1970s to reproduce the decreasing trend. However, more information is required to further improve the emission inventory on fuel consumption and technology level. With the method developed in this work, we will use measurement data from multiple states to constrain historical emission from different fuel-technology sources. Identifying the fuel-use and emission factors that need adjustment will ultimately improve emission estimates of BC and other species[20].

REFERENCES

1.	Bond, T.C., et al., *Bounding the role of black carbon in the climate system: A scientific assessment.* Journal of Geophysical Research: Atmospheres, 2013. 118(11): p. 5380-5552.

2.	Bond, T.C., et al., *Historical emissions of black and organic carbon aerosol from energy-related combustion, 1850–2000.* Global Biogeochemical Cycles, 2007. 21(2): p. GB2018.

3.	Dickerson, R.R., et al., *Analysis of black carbon and carbon monoxide observed over the Indian Ocean: Implications for emissions and photochemistry.* Journal of Geophysical Research: Atmospheres, 2002. 107(D19): p. 8017.

4.	Bond, T.C., et al., *Quantifying immediate radiative forcing by black carbon and organic matter with the Specific Forcing Pulse.* Atmos. Chem. Phys., 2011. 11(4): p. 1505-1525.

5.	Schulz, M., et al., *Radiative forcing by aerosols as derived from the AeroCom present-day and pre-industrial simulations.* Atmos. Chem. Phys., 2006. 6(12): p. 5225-5246.

6.	Hansen, J.E. and M. Sato, *Trends of measured climate forcing agents.* Proceedings of the National Academy of Sciences, 2001. 98(26): p. 14778-14783.

7.   Smith, S.J., T.M.L. Wigley, and J. Edmonds, *A New Route Toward Limiting Climate Change?* Science, 2000. 290(5494): p. 1109-1110.

8.   Zhang, H., et al., *Simulation of direct radiative forcing of aerosols and their effects on East Asian climate using an interactive AGCM-aerosol coupled system.* Climate Dynamics, 2012. 38(7-8): p. 1675-1693.

9.   Chung, S.H. and J.H. Seinfeld, *Global distribution and climate forcing of carbonaceous aerosols.* Journal of Geophysical Research: Atmospheres (1984–2012), 2002. 107(D19): p. AAC 14-1-AAC 14-33.

10.   Jacob, D.J. *Lectures on inverse modeling.* 2007.

11.   Wang, Y., et al., *Black carbon and its correlation with trace gases at a rural site in Beijing: Top-down constraints from ambient measurements on bottom-up emissions.* Journal of Geophysical Research: Atmospheres, 2011. 116(D24): p. D24304.

12.   Lamarque, J.F., et al., *Historical (1850–2000) gridded anthropogenic and biomass burning emissions of reactive gases and aerosols: methodology and application.* Atmos. Chem. Phys., 2010. 10(15): p. 7017-7039.

13.   Yan, F., et al., *Global emission projections of particulate matter (PM): I. Exhaust emissions from on-road vehicles.* Atmospheric Environment, 2011. 45(28): p. 4830-4844.

14.   Quayle, R.G. and H.F. Diaz, *Heating degree day data applied to residential heating energy consumption.* Journal of Applied Meteorology, 1980. 19(3): p. 241-246.

15.   Kaynakli, O., *A study on residential heating energy requirement and optimum insulation thickness.* Renewable Energy, 2008. 33(6): p. 1164-1172.

16.   Stohl, A., et al., *Black carbon in the Arctic: the underestimated role of gas flaring and residential combustion emissions.* Atmos. Chem. Phys., 2013. 13(17): p. 8833-8855.

17.   Hansen, A., H. Rosen, and T. Novakov, *The aethalometer—an instrument for the real-time measurement of optical absorption by aerosol particles.* Science of the Total Environment, 1984. 36: p. 191-196.

18.   Kirchstetter, T.W., et al., *Black carbon concentrations and diesel vehicle emission factors derived from coefficient of haze measurements in California: 1967–2003.* Atmospheric Environment, 2008. 42(3): p. 480-491.

19.   Allen, G.A., J. Lawrence, and P. Koutrakis, *Field validation of a semi-continuous method for aerosol black carbon (aethalometer) and temporal patterns of summertime hourly black carbon measurements in southwestern PA.* Atmospheric Environment, 1999. 33(5): p. 817-823.

20.   Sun, T., Liu, L., Bond, T.C., Flanner, M., Kirchstetter T.W., Jiao, C., Preble, C.V., Chang W.,, *Constraining historical black carbon emission inventory of United States for 1960s-2000s.* To be published work.

KEY WORDS

Emission Inventory
Black Carbon
Inverse modeling

SUPPLEMENTARY INFORMATION

1. Full transport matrix

Table S1. Transport matrix with the receptor region of California and 23 global emission source regions

T matrix (µg/m³)/Gg	Jan	Feb	Mar	Apr	May	Jun	Jul	Aug	Sep	Oct	Nov	Dec
Canada	5.12E-05	1.43E-04	1.58E-04	3.00E-04	3.67E-04	6.20E-04	8.65E-04	1.02E-03	9.01E-04	4.56E-04	1.10E-04	6.31E-05
USA	2.21E-02	1.76E-02	1.58E-02	1.35E-02	1.56E-02	1.70E-02	1.93E-02	2.06E-02	2.16E-02	2.18E-02	2.15E-02	2.23E-02
Central America	4.49E-03	3.54E-03	2.76E-03	2.31E-03	2.59E-03	2.79E-03	3.18E-03	3.38E-03	3.53E-03	3.75E-03	4.18E-03	4.74E-03
South America	1.02E-06	6.29E-07	8.35E-07	8.49E-07	1.10E-06	9.30E-07	2.43E-06	3.70E-06	2.28E-06	1.00E-06	5.02E-07	5.60E-07
Northern Africa	6.41E-06	6.80E-06	1.16E-05	1.45E-05	1.58E-05	7.94E-06	4.81E-06	5.46E-06	9.55E-06	1.53E-05	1.52E-05	1.02E-05
Western Africa	4.10E-06	2.35E-06	3.87E-06	3.51E-06	3.17E-06	1.63E-06	3.29E-06	3.03E-06	2.81E-06	2.21E-06	2.95E-06	3.19E-06
Eastern Africa	3.56E-06	2.08E-06	3.53E-06	3.69E-06	2.99E-06	8.79E-07	7.05E-07	9.44E-07	1.34E-06	1.33E-06	2.16E-06	2.37E-06
Southern Africa	5.55E-07	3.46E-07	5.06E-07	3.18E-07	2.80E-07	1.75E-07	1.39E-07	1.38E-07	1.15E-07	7.17E-08	6.89E-08	1.64E-07
OECD Europe	3.57E-06	3.87E-06	8.53E-06	1.26E-05	1.80E-05	1.70E-05	1.30E-05	1.67E-05	2.48E-05	1.88E-05	1.21E-05	5.55E-06
Eastern Europe	1.74E-06	2.49E-06	5.81E-06	1.53E-05	2.88E-05	2.77E-05	1.80E-05	2.34E-05	3.18E-05	2.10E-05	9.14E-06	3.12E-06
Former USSR	1.80E-06	2.24E-06	5.33E-06	1.28E-05	3.76E-05	5.03E-05	3.42E-05	3.75E-05	4.33E-05	2.02E-05	7.24E-06	2.79E-06
Middle East	7.52E-06	9.73E-06	2.01E-05	2.99E-05	3.54E-05	1.93E-05	9.90E-06	9.58E-06	1.70E-05	2.35E-05	2.39E-05	1.21E-05
South Asia	9.00E-06	1.12E-05	2.03E-05	2.27E-05	2.48E-05	1.24E-05	5.56E-06	4.50E-06	7.36E-06	1.21E-05	1.00E-05	6.60E-06
East Asia	1.78E-05	1.71E-05	4.00E-05	6.48E-05	8.43E-05	9.00E-05	6.45E-05	4.78E-05	4.71E-05	4.53E-05	2.51E-05	1.70E-05
Southeat Asia	7.66E-06	6.64E-06	1.36E-05	1.36E-05	1.73E-05	8.60E-06	5.65E-06	3.26E-06	3.12E-06	4.82E-06	5.32E-06	5.46E-06
Oceania	3.66E-08	3.42E-08	5.84E-08	4.69E-08	4.89E-08	3.80E-08	2.74E-08	1.95E-08	1.91E-08	1.33E-08	1.38E-08	1.92E-08
Japan	8.72E-05	7.65E-05	9.81E-05	1.10E-04	1.20E-04	1.27E-04	1.39E-04	1.21E-04	1.21E-04	9.56E-05	8.69E-05	8.41E-05
Euro Biomass	6.73E-06	2.69E-06	3.76E-06	7.72E-06	6.23E-05	4.98E-05	7.00E-06	8.72E-06	4.77E-05	8.44E-05	4.45E-05	9.64E-06
Northern Asia Biomass	5.63E-05	2.34E-05	7.57E-06	2.03E-05	6.31E-05	2.04E-04	7.59E-05	9.04E-05	1.40E-04	3.13E-05	6.49E-05	8.93E-05
Southern Asia Biomass	1.97E-06	3.64E-06	1.42E-05	2.74E-05	5.94E-05	7.66E-06	6.04E-06	1.88E-06	1.63E-06	1.21E-06	1.51E-06	1.29E-06
North America Biomass	1.07E-02	7.89E-03	1.07E-02	7.61E-03	8.03E-03	2.83E-03	5.17E-03	8.79E-03	4.09E-02	2.16E-02	1.07E-02	1.86E-02
S/C America Biomass	4.46E-06	1.27E-06	1.27E-06	3.80E-06	2.00E-05	1.76E-05	1.35E-05	1.67E-06	7.84E-07	1.15E-06	2.13E-06	2.58E-06

T matrix (µg/m³)/Gg	Jan	Feb	Mar	Apr	May	Jun	Jul	Aug	Sep	Oct	Nov	Dec
Africa Biomass	2.75E-06	2.27E-06	1.47E-05	1.18E-05	1.10E-06	1.82E-07	1.36E-07	1.98E-07	2.20E-07	3.09E-07	1.22E-06	1.45E-06

2. Seasonality of HDD for California

Seasonality of HDD for California is calculated based on Equation (3).
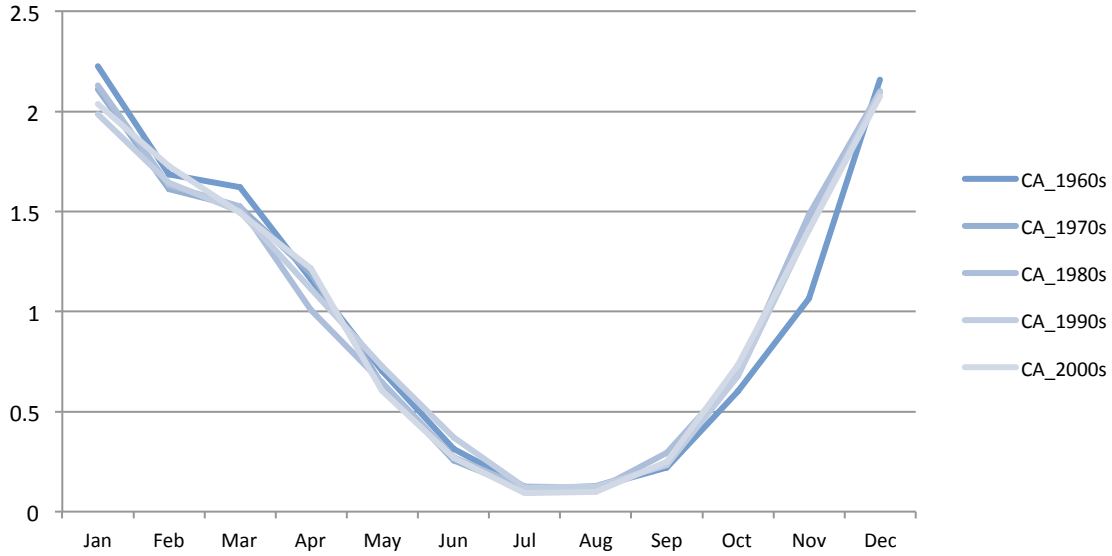
Figure S1. Seasonality of HDD for California over each decade during 1960s-2000s. Data are calculated from National Oceanic and Atmospheric Administration (NOAA) National Climate Data Center

3. Adjustment of baseline and seasonal emission

For the ith month:

Equation (S1) $\overline{R_i} = \dfrac{\overline{C_{mi}}}{\overline{C_{ei}}} = \dfrac{E'_b + \overline{E'_{si}}}{E_b + \overline{E_{s_1}}}$ for i^{th} month

Equation (S2) $R_{summer} = \dfrac{C_{mi}}{C_{ei}} = \dfrac{E'_b}{E_b}$ for $i = 6,7,8$

Equation (S3) $\dfrac{E_b}{E_{s_1}} = k$

Equation (S4) $E'_b = R_{summer} E_b$

Equation (S5) $\overline{E_{s_1}'} = (k(\overline{R_i} - R_{summer}) + \overline{R_i})\,\overline{E_{s_1}}$

where C_{mi} and C_{ei} are the measured and estimated BC concentrations for each month. E'_b and E_b are the true and estimated baseline emissions, respectively. E_{s_i}' and E_{s_i} are the true and estimated seasonal emissions for each month. R_i, R_{summer} and k are intermediate variable.

The ratio between the measured BC concentrations and the modeled BC concentrations for each month, following adjustments for model errors, should be equal to the ratio of true BC emissions to estimated emissions, as shown by Equation (5). Meanwhile, we assumed that only baseline emissions occur in summer. Therefore, adjustment to the baseline and seasonal emissions can be calculated with the observation as Equation S4, S5 demonstrated.